ELECTRONIC SUPPLEMENTARY INFORMATION (ESI)

Polymerization of Ethylene and Propylene Promoted by Group 4 Metal Complexes Bearing Thioetherphenolate Ligands

Ermanno Luciano,[a] Francesco Della Monica,[a] Antonio Buonerba,[a] Alfonso Grassi,[a] Carmine Capacchione[a]* and Stefano Milione[a]

[a] *Dipartimento di Chimica e Biologia and NANOMATES Research Centre for NANOMAterials and nanoTEchnology, Università degli Studi di Salerno, via Giovanni Paolo II 132 - 84084 Fisciano (SA).*

* *E-mail: ccapacchione@unisa.it.*

Table of Contents

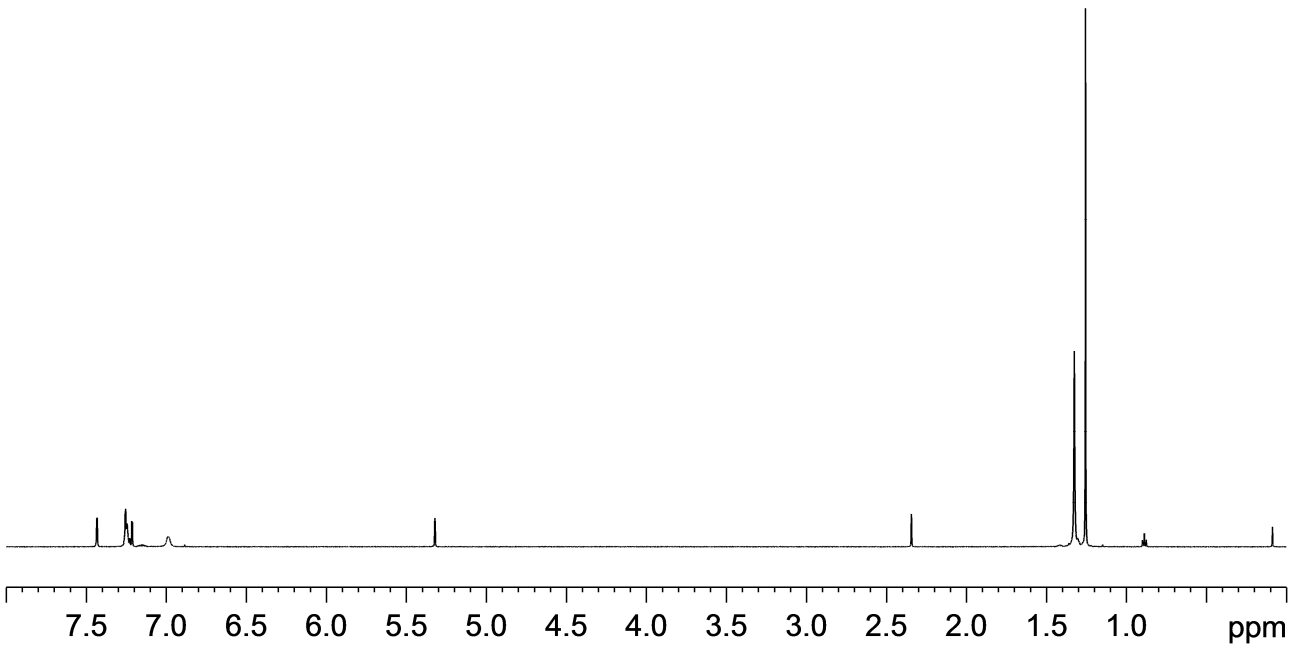

Figure S1. ^{1}H NMR spectrum (CD_2Cl_2, 25 °C, 600 MHz) of complex ($^{t\text{-Bu}}$OS)$_2$TiCl$_2$ (**1**).

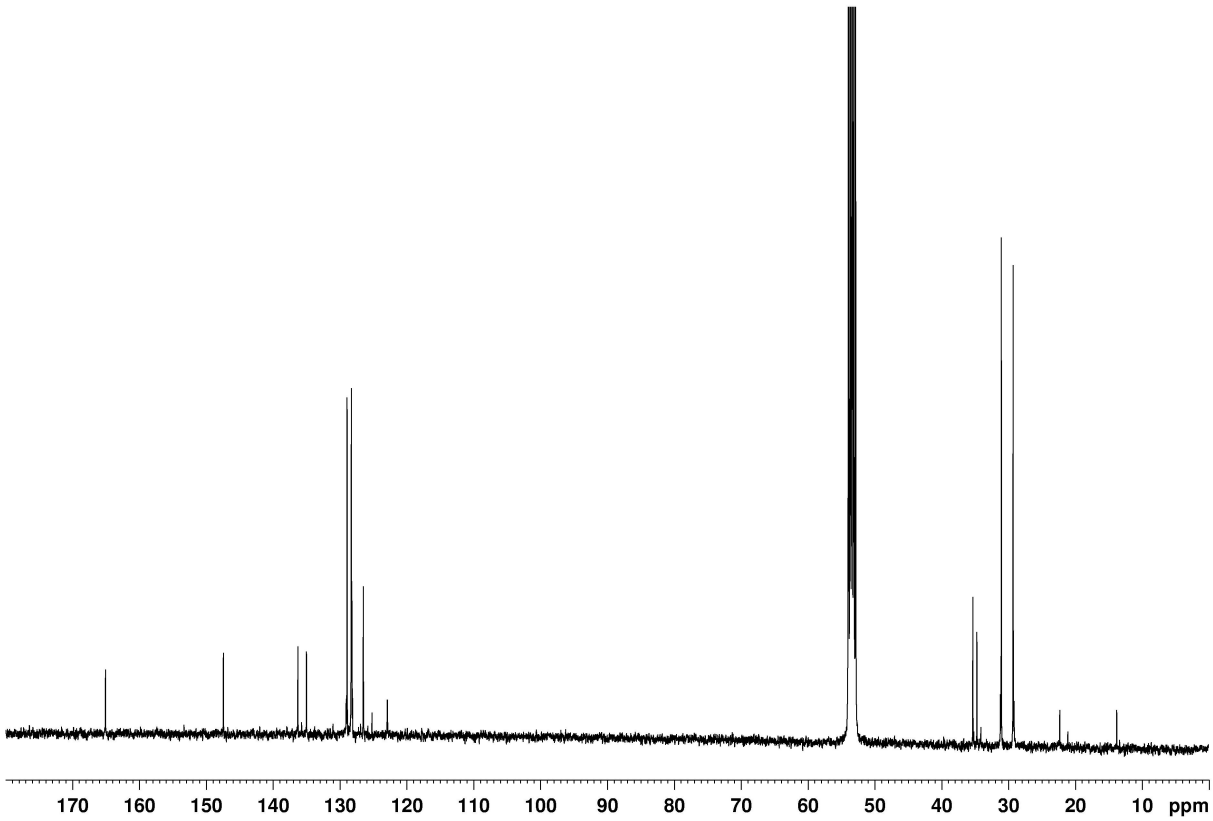

Figure S2. ^{13}C NMR spectrum (CD_2Cl_2, 25 °C, 100 MHz) of complex ($^{t\text{-Bu}}$OS)$_2$TiCl$_2$ (**1**).

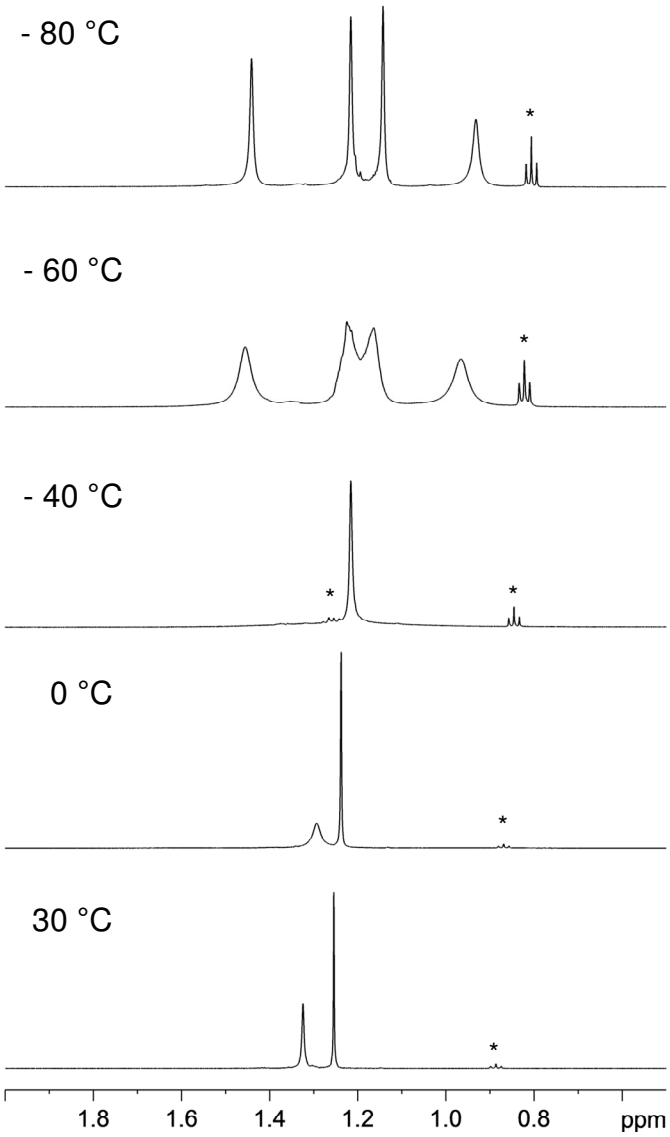

Figure S3. Variable-temperature ^{1}H NMR spectra (CD_2Cl_2, 600 MHz) of complex ($^{t\text{-Bu}}$OS)$_2$TiCl$_2$ (**1**). The signals marked with an asterisk are due to pentane impurity.

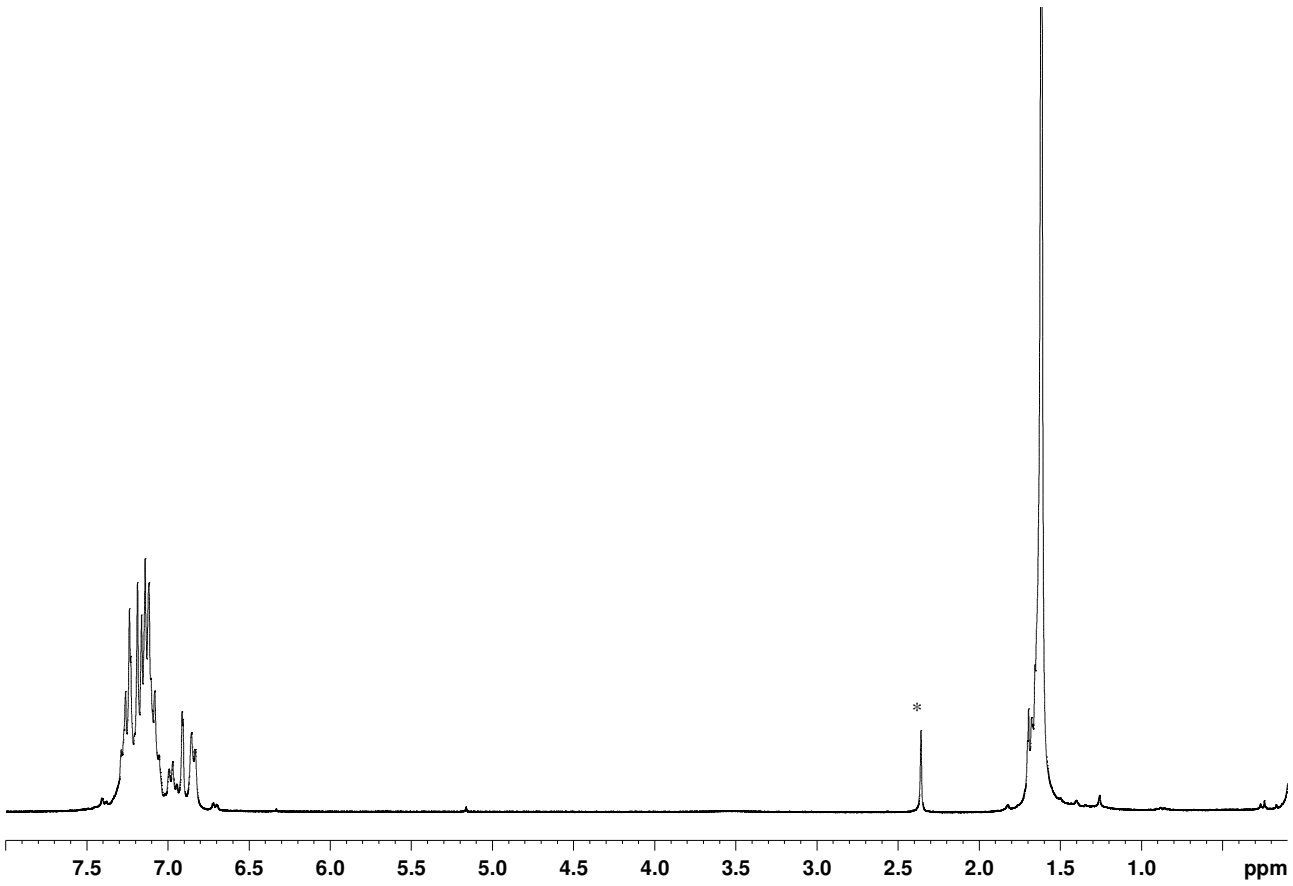

Figure S4. ^{1}H NMR spectrum ($CDCl_3$, 25 °C, 400 MHz) of complex $(^{Cum}OS)_2TiCl_2$ (**2**)(* = toluene).

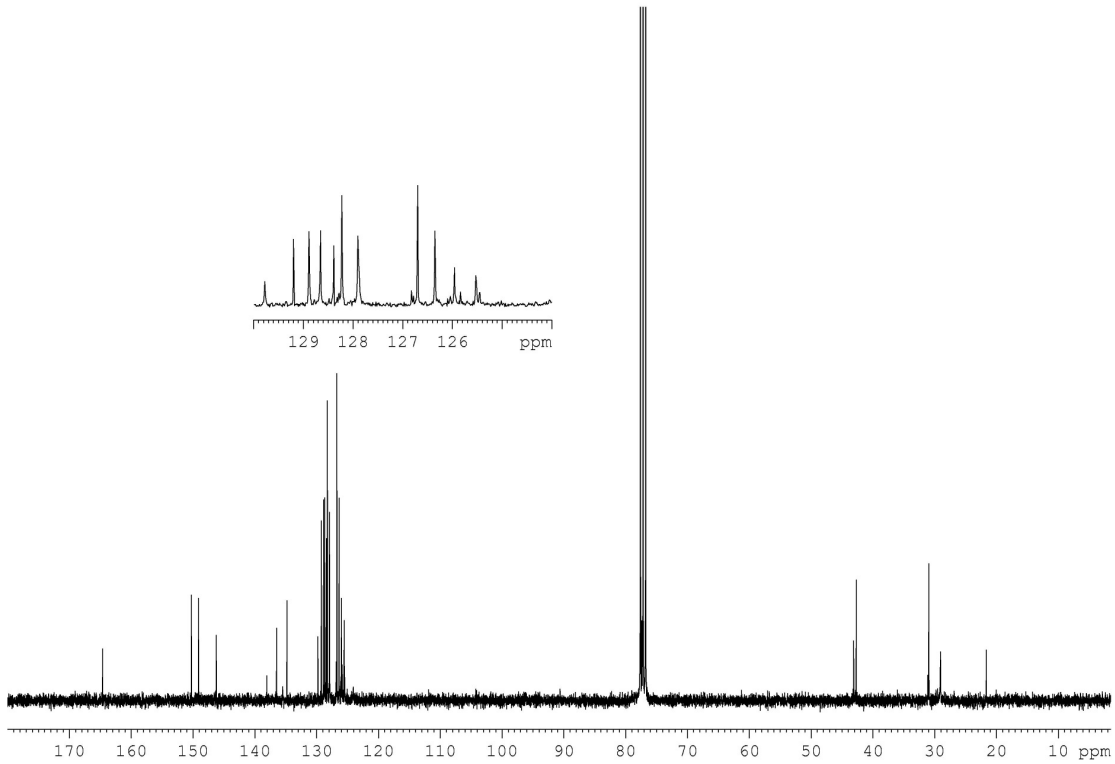

Figure S5. ^{13}C NMR spectrum ($CDCl_3$, 25 °C, 75 MHz) of complex $(^{Cum}OS)_2TiCl_2$ (**2**).

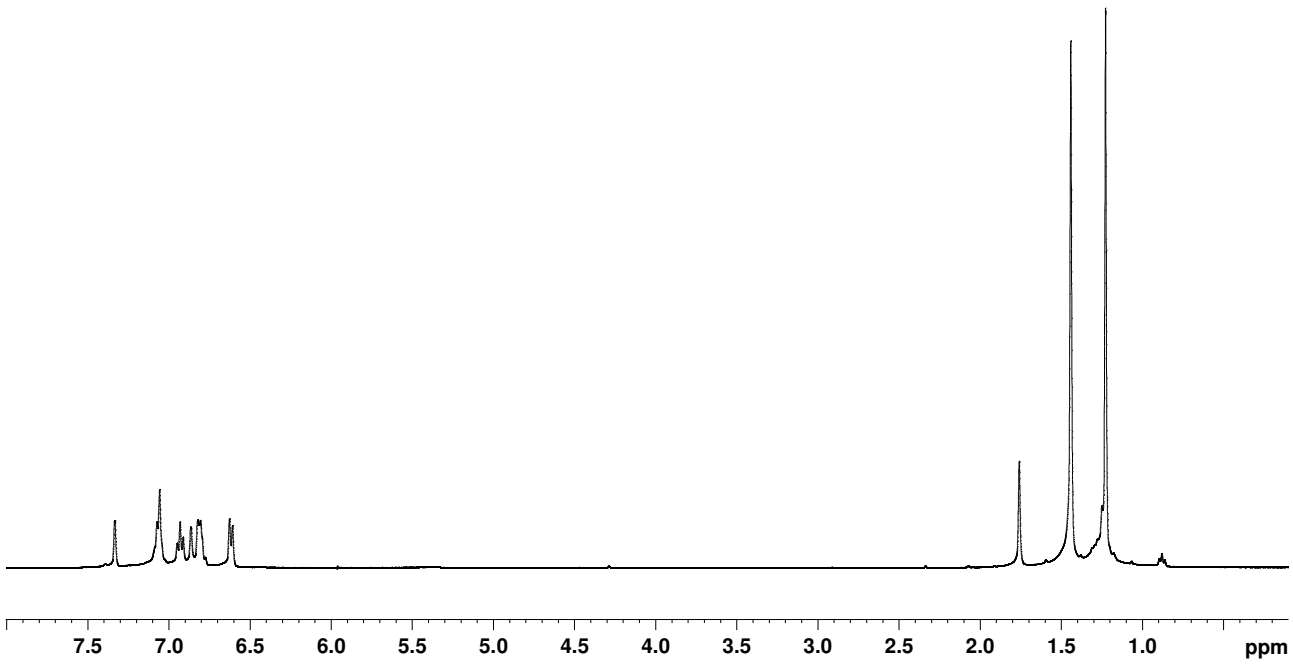

Figure S6. ^{1}H NMR spectrum (CD_2Cl_2, 25 °C, 400 MHz) of complex ($^{t\text{-Bu}}$OS)$_2$ZrBn$_2$ (**3**).

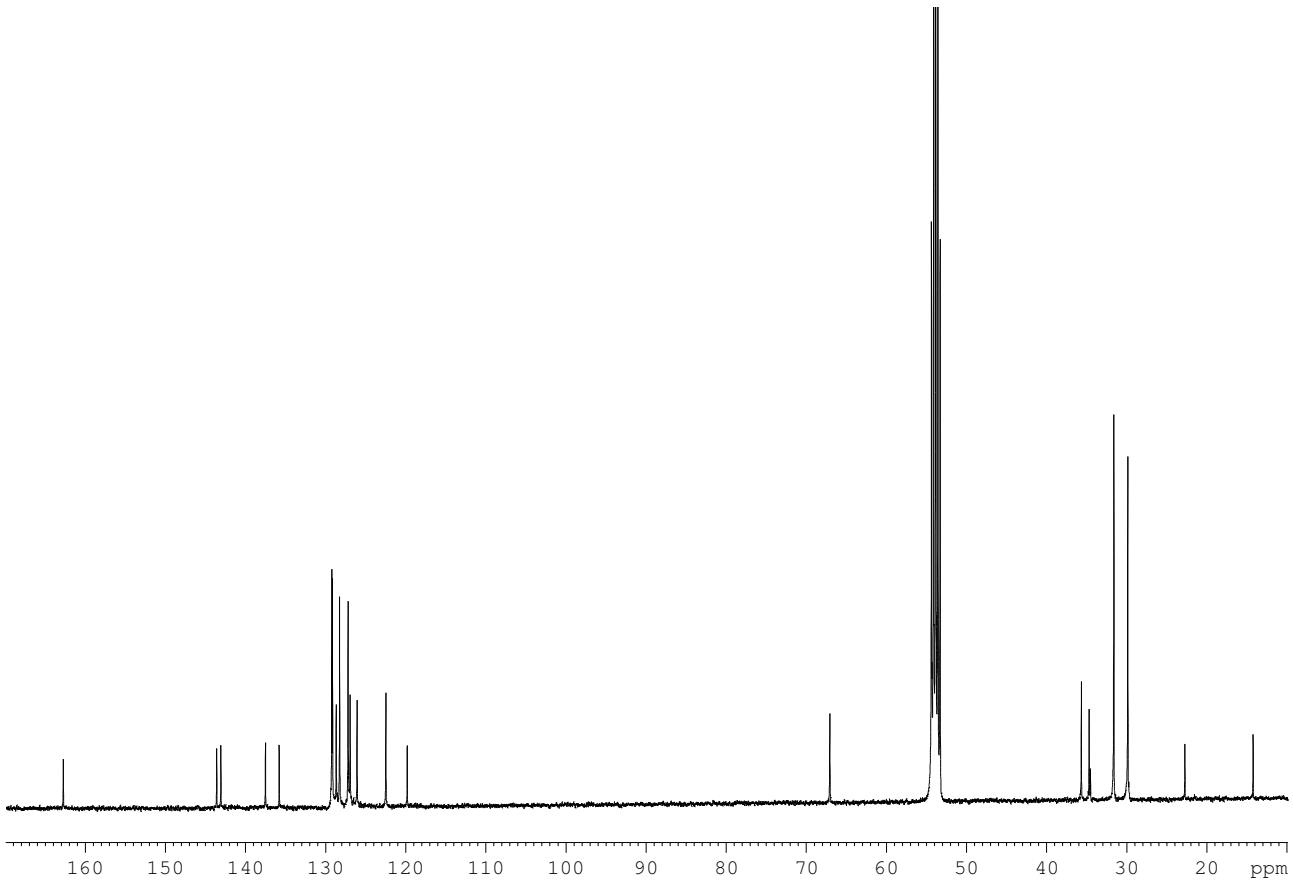

Figure S7. ^{13}C NMR spectrum (CD_2Cl_2, 25 °C, 100 MHz) of complex ($^{t\text{-Bu}}$OS)$_2$ZrBn$_2$ (**3**).

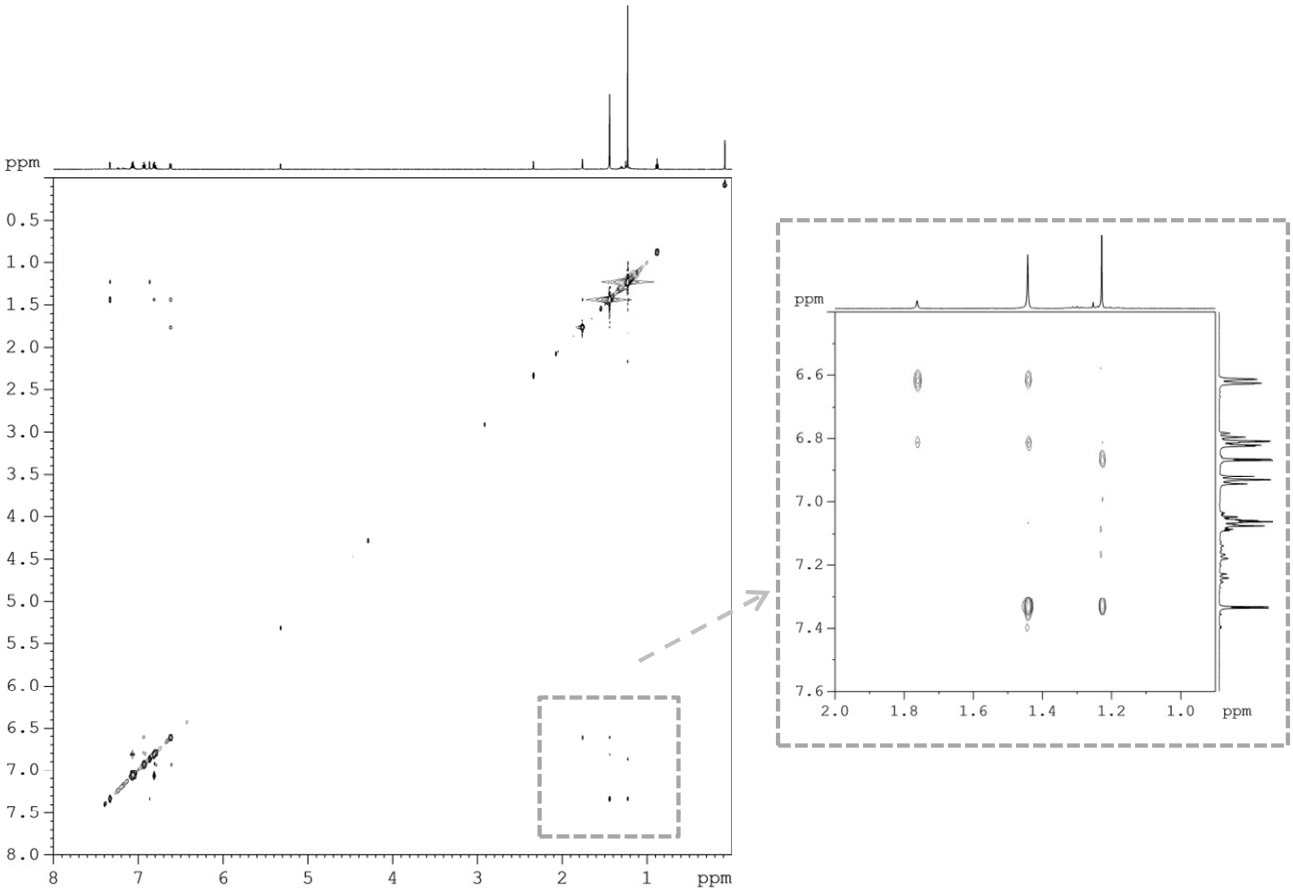

Figure S8. ^{1}H-^{1}H NOESY spectrum (τ_m = 0.400 s, CD_2Cl_2, 600 MHz) of complex $(^{t\text{-Bu}}OS)_2ZrBn_2$ (**3**) at room temperature.

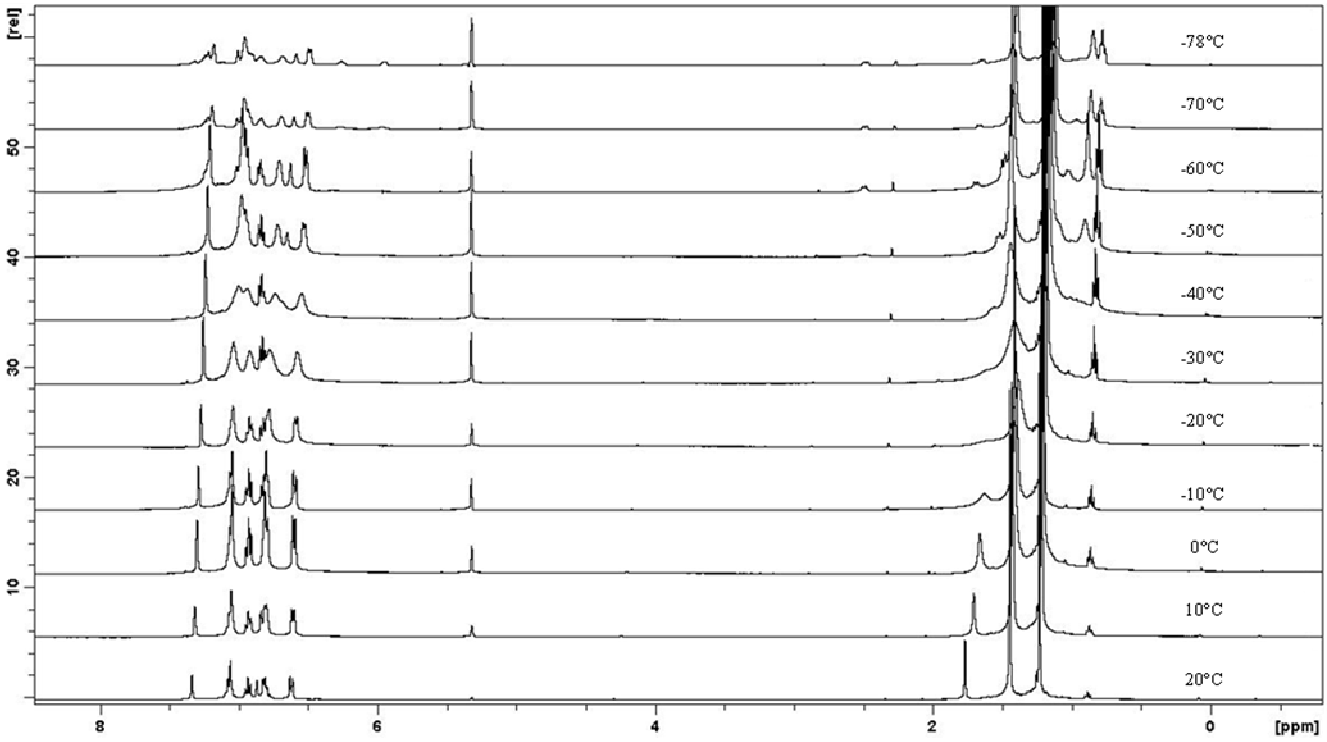

Figure S9a. Variable-temperature ^{1}H NMR spectra (CD_2Cl_2, 400 MHz) of complex ($^{t\text{-Bu}}$OS)$_2$ZrBn$_2$ (**3**).

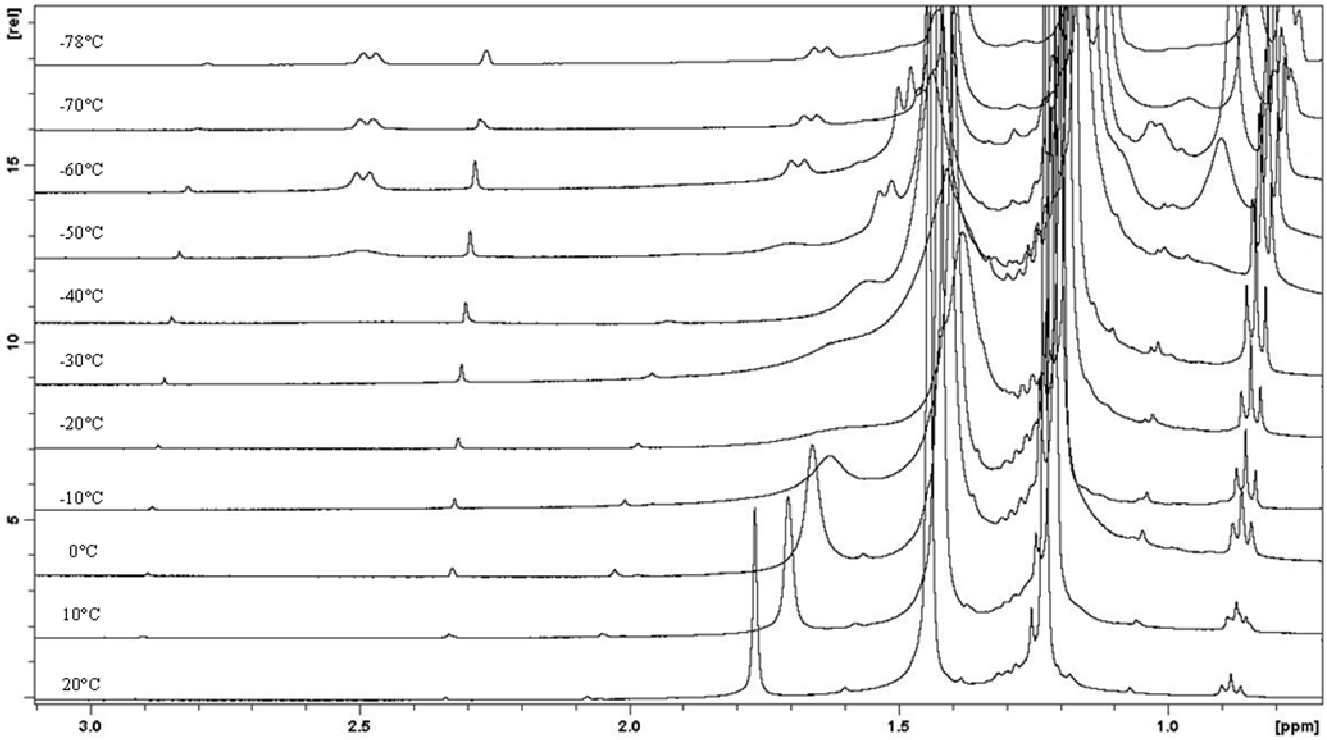

Figure S9b. Variable-temperature ^{1}H NMR spectra (CD_2Cl_2, 400 MHz) of complex ($^{t\text{-Bu}}$OS)$_2$ZrBn$_2$ (**3**).in the region from 0.7 to 3.1 ppm.

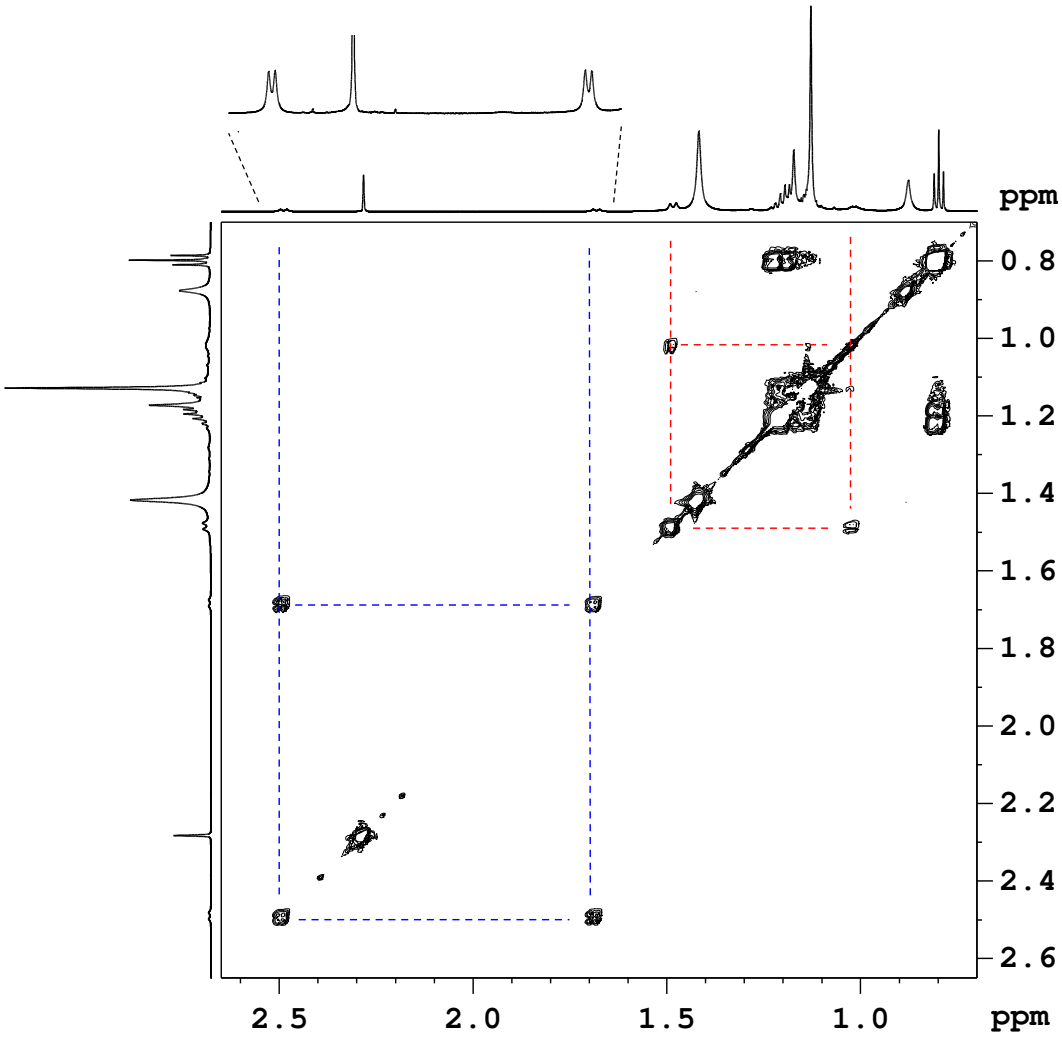

Figure S10. COSY spectrum (CD_2Cl_2, 600MHz) of complex ($(^{t\text{-Bu}}OS)_2ZrBn_2$ (**3**) showing the scalar coupling of the Zr-CH_2-Ph resonances at -80 °C.

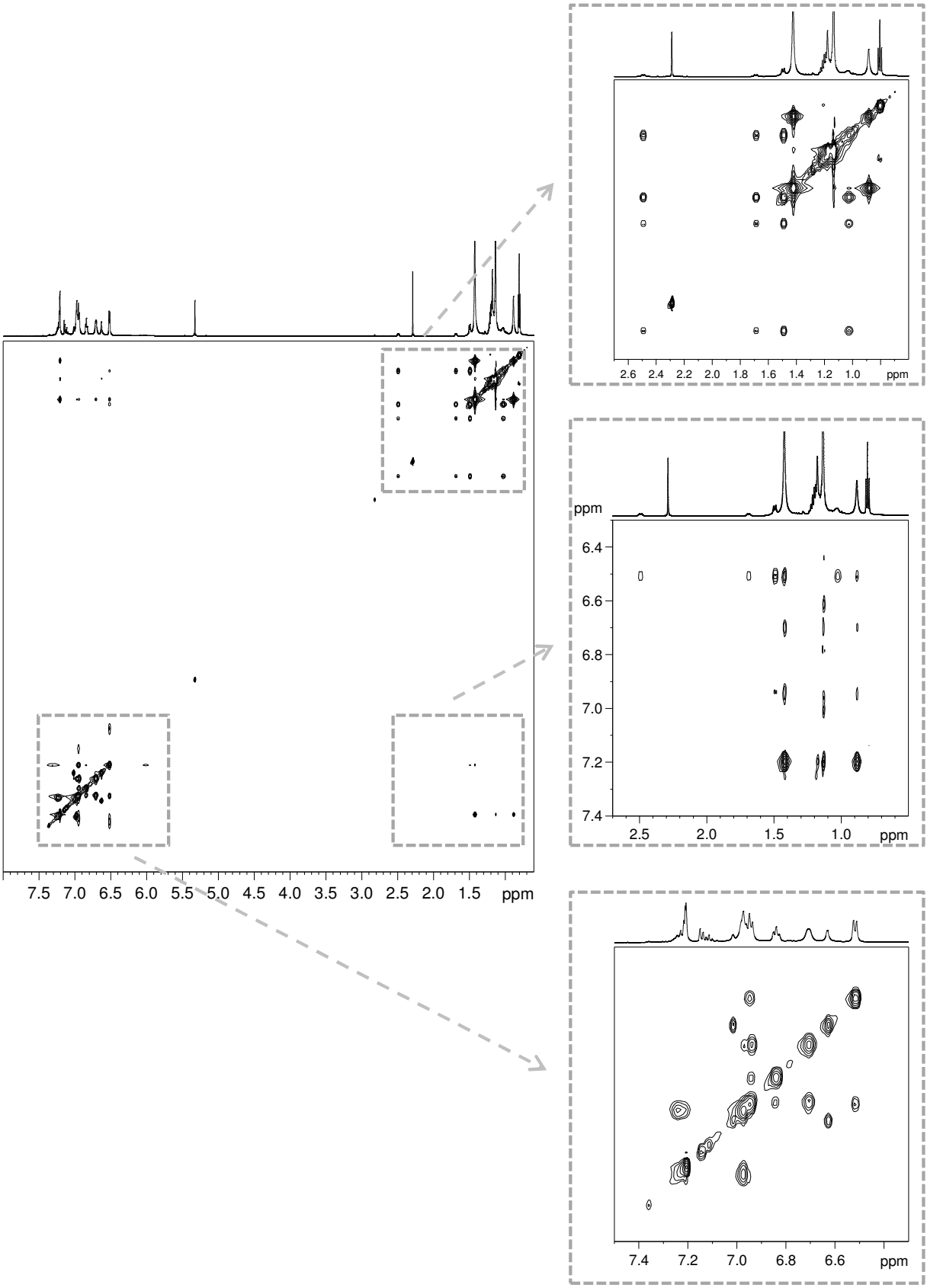

Figure S11. ^{1}H-^{1}H NOESY spectrum (τ_m = 0.400 s, CD_2Cl_2, 600 MHz) of complex $(^{t\text{-Bu}}OS)_2ZrBn_2$ (**3**) at -80 °C.

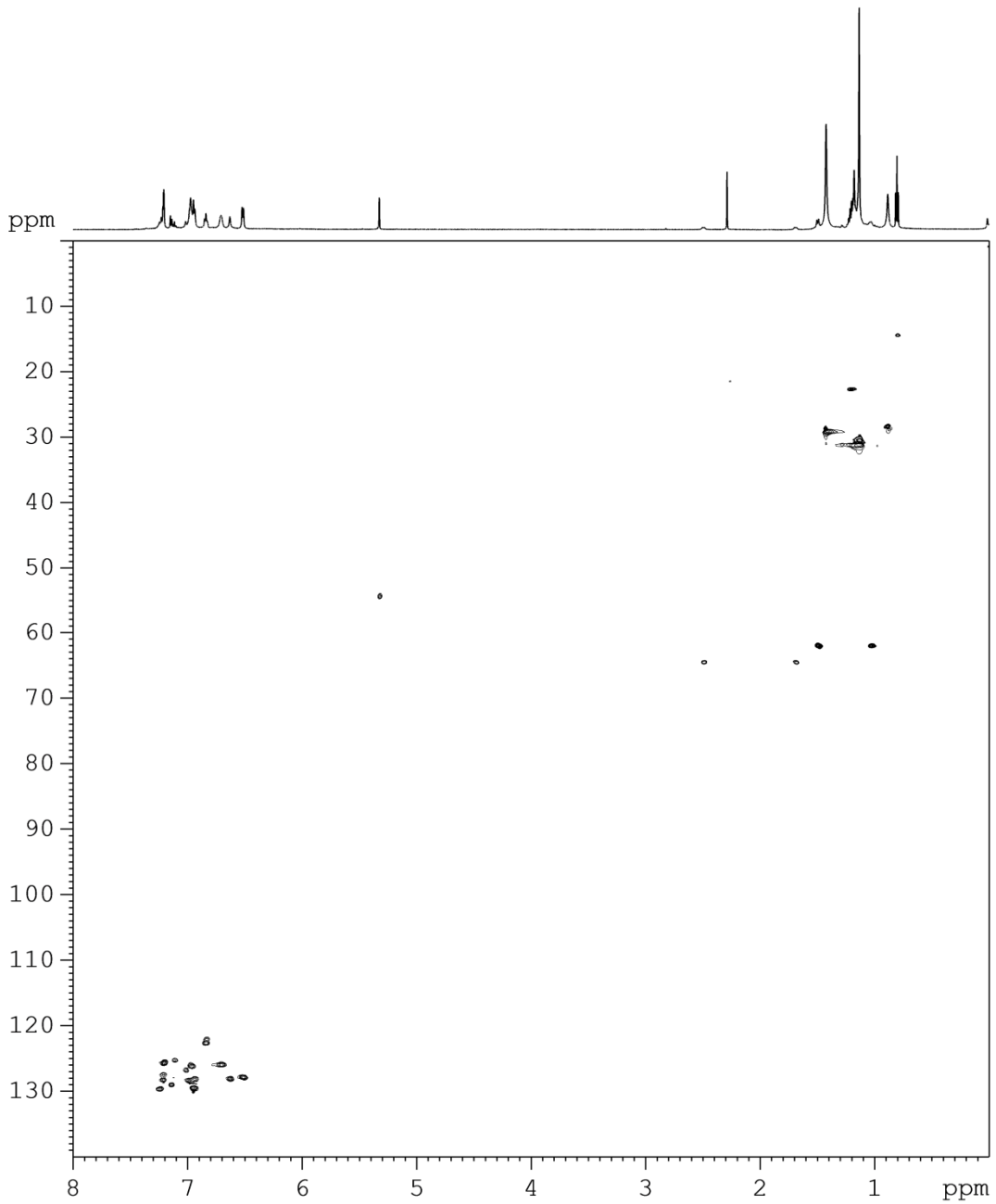

Figure S12. ^{1}H-^{13}C HSQC spectrum (CD_2Cl_2, 600 MHz) of complex ($(^{t\text{-Bu}}OS)_2ZrBn_2$ (**3**) at -80 °C.

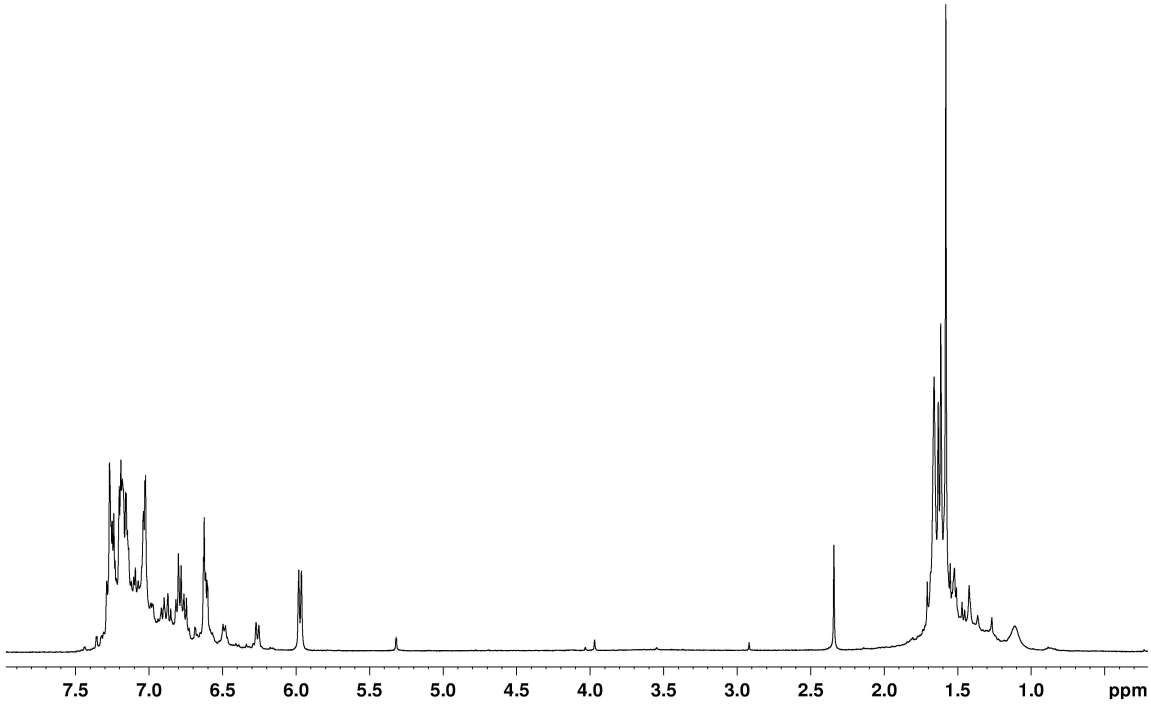

Figure S13. ^{1}H NMR spectrum (CD_2Cl_2, 25 °C, 400 MHz) of complex ($^{Cum}OS)_2ZrBn_2$ (**4**).

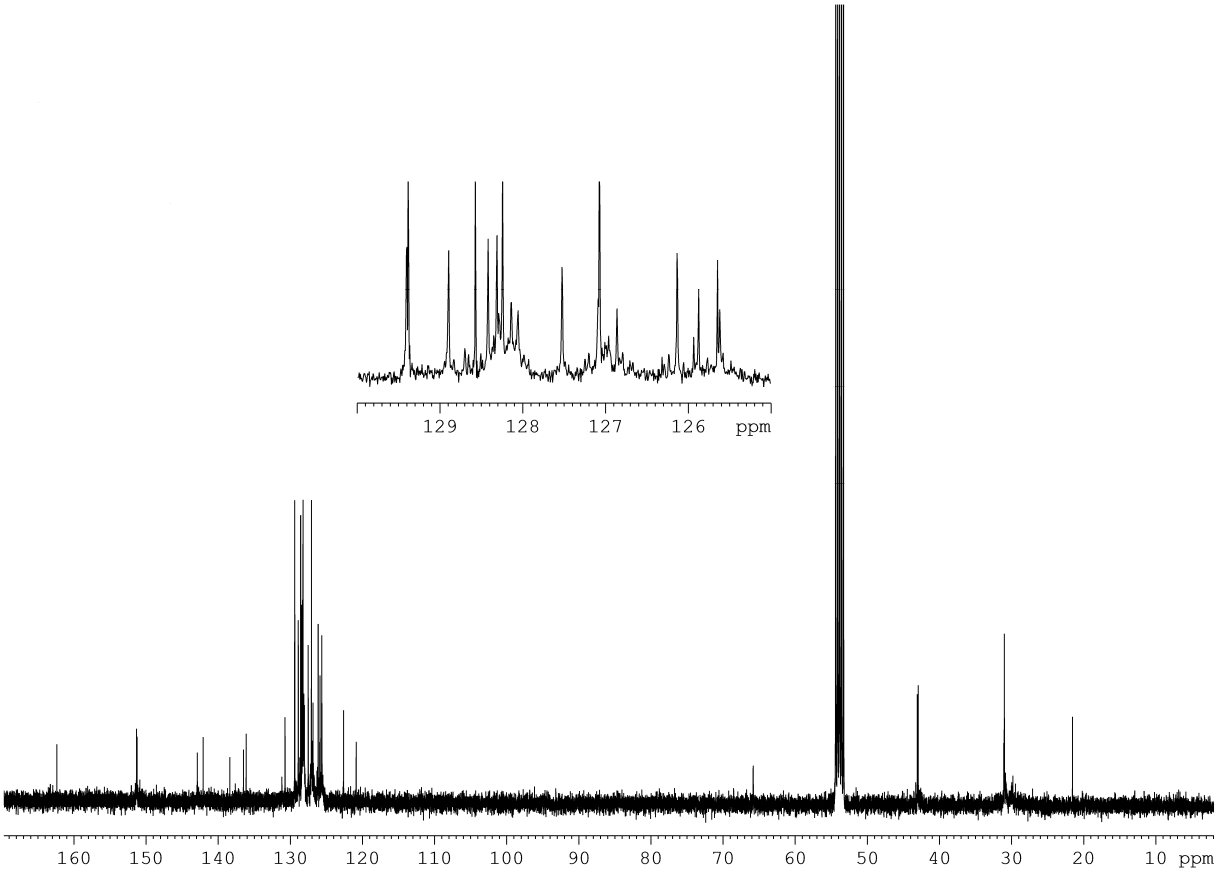

Figure S14. ^{13}C NMR spectrum (CD_2Cl_2, 25 °C, 75 MHz) of complex ($^{Cum}OS)_2ZrBn_2$ (**4**).

Table S1. Internal and Free Energy differences (kcal/mol) of the minimum energy structures for the five diastereoisomers of the $(OS)_2MX_2$ complexes (M = Ti, X = Cl; M = Zr, X = Me).

		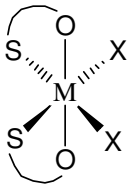	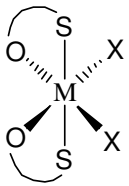	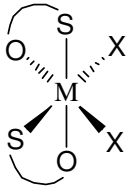	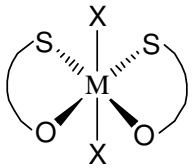	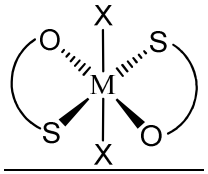
	Diasteroisomer	A	B	C	D	E
	Symmetry	C_2	C_2	C_1	C_2	C_i
Titanium	Minimum Energy structure	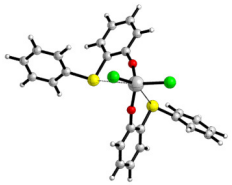	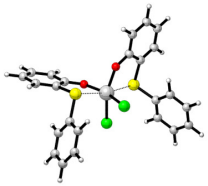	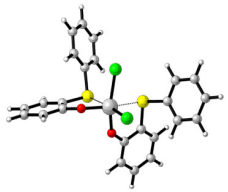	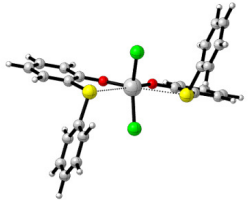	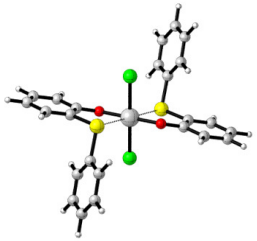
	Imag. freq.[a]	0	0	0	0	2
	ΔE	0.0	3.9	-1.7	0.4	15.5
	ΔE_{ZPE}[b]	0.0	3.5	-1.8	0.3	-
	ΔG[c]	0.0	8.3	3.9	4.8	-
Zirconium	Minimum Energy structure	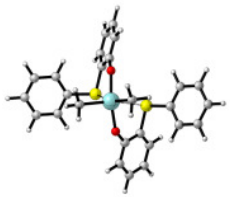	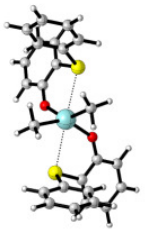	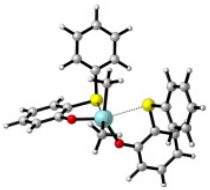	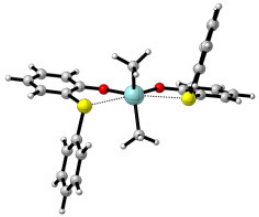	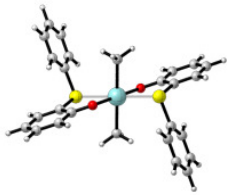
	Imag. freq.[a]	0	0	0	0	3
	ΔE	0.0	3.8	2.0	2.7	37.6
	ΔE_{ZPE}[b]	0.0	4.5	2.3	3.0	-
	ΔG[c]	0.0	6.2	3.0	4.5	-

[a] Number of imaginary frequencies [b] Zero Point Energy (ZPE) Corrected Energies (at 0 K); [c] Free Energies in gas phase thermodynamically corrected to 298 K.

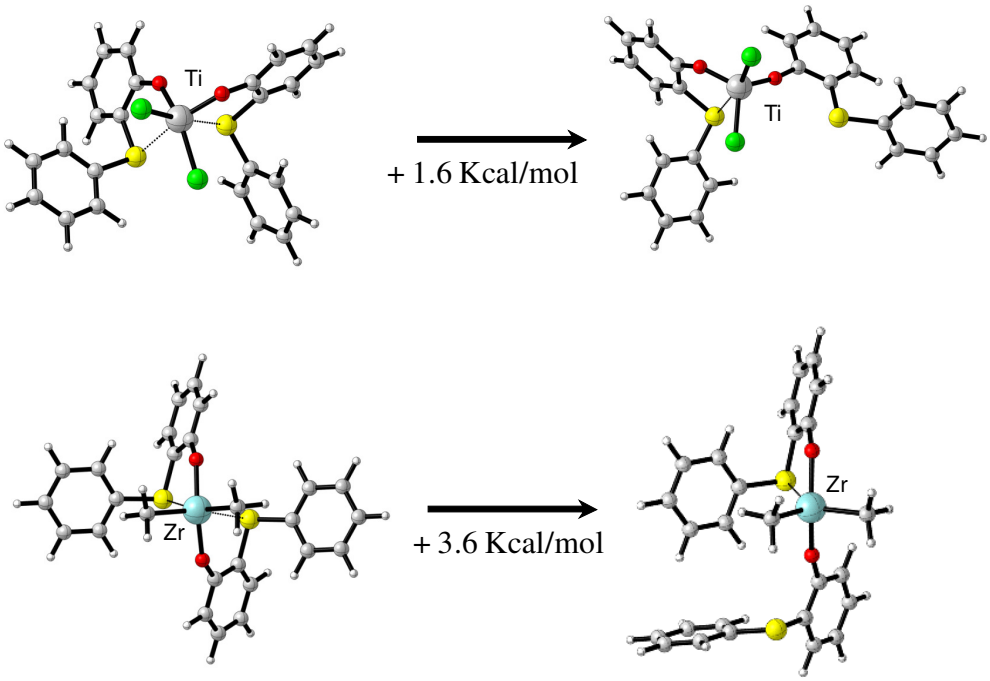

Figure S15. The opening ($\kappa^2 \rightarrow \kappa^1$) of one of the OS ligands in the titanium and zirconium $(OS)_2TiCl_2$ and $(OS)_2ZrMe_2$ complexes. The stereoisomers C and A were considered as starting species for the titanium and zirconium complexes, respectively.

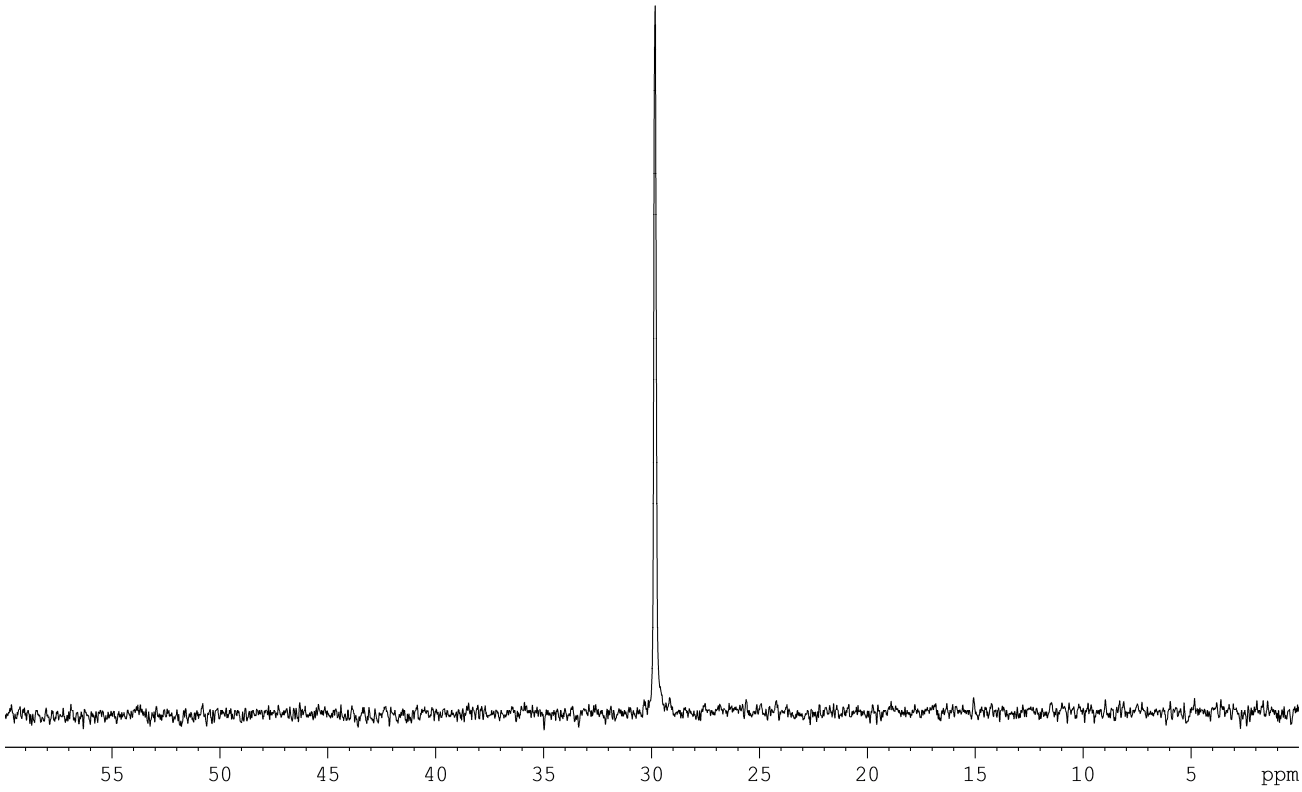

Figure S16. ^{13}C NMR spectrum (TCDE, 110°C, 75 MHz) of polyethylene of run 1, Table 1.

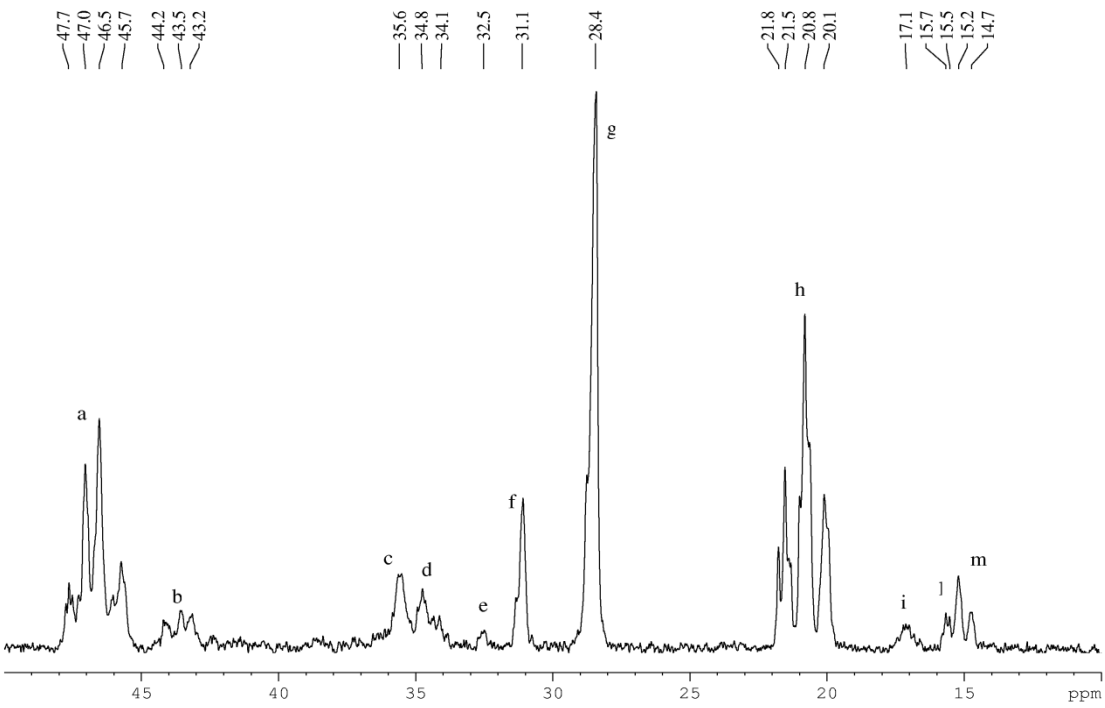

Figure S17. Aliphatic region of ^{13}C NMR spectrum (TCDE, 110°C, 75 MHz) of polypropylene sample of run 1 in Table 2.

Table S2. ^{13}C NMR chemical shift of polypropylene sample and the corresponding literature values for regioirregular polypropylene.[1]

Line	Chemical shift (ppm from TMS)		H-T	H-H	T-T	1-r
	exp	Literature[1]				
a	45.7-47.6	45.7-47.7	$S_{\gamma\alpha\alpha\gamma}$ (1)			
		45.7-46.5			$S_{\gamma\alpha\alpha\delta}$ (7)	
b	42.9-44.2	43.3-44.1		r_0-$S_{\beta\alpha\alpha\gamma}$ (4)		r_0-$S_{\beta\alpha\alpha\gamma}$ (19)
		40.9-42.3		m_0-$S_{\beta\alpha\alpha\gamma}$ (4)		
		36.8-39.1				r_0-$T_{\delta\gamma\alpha\gamma}$ (15)
		36.5				r_1-$S_{\gamma\alpha\beta\gamma}$ (13)
c	35.6	35.4-35.6		m_0-$T_{\alpha\beta}$ (5)	r_1-$S_{\gamma\alpha\beta\delta}$ (10)	m_1-$S_{\gamma\alpha\beta\gamma}$ (13)
d	34.1-34.8	34.2-34.8		r_0-$T_{\alpha\beta}$ (5)	m_1-$S_{\gamma\alpha\beta\delta}$ (10)	r_0-$T_{\delta\alpha\beta\delta}$ (17)
e	32.6	32.6				r_0-$S_{\delta\beta\alpha\beta}$ (14)
f	31.1	31.1-31.3			$T_{\delta\beta\gamma\delta+}$ (8)	$T_{\delta\beta\gamma\delta}$ (11)
g	28.4	28.3-28.4	$T_{\beta\beta}$ (2)			
h	20.1-21.8	20.1-21.7	$P_{\beta\beta}$ (3)			
		20.1-20.9			m_1-$P_{\beta\gamma}$ (9) r_1-$P_{\beta\gamma}$ (9)	m_1-$P_{\delta\beta\gamma\delta}$ (12) r_1-$P_{\delta\beta\gamma\delta}$ (12)
i	16.8-17.2	16.6-17.2		m_0-$P_{\alpha\beta}$ (6)		
l	15.5-17.5					
m	14.7-15.2	14.7-15.1		r_0-$P_{\alpha\beta}$ (6)		r_0-$P_{\delta\gamma\alpha\gamma}$ (16) r_0-$P_{\delta\alpha\beta\delta}$ (18)

The table contains the chemical shifts of peaks observed in the ^{13}C spectrum of PP obtained from run 1 Table2. The observed chemical shifts are listed in the column **exp**, and compared to those reported in literature and listed in the column **Literature**. The letters in column **Line** refer to Figure S17 and the numbers reported in brackets refer to the Figure S18.

1) Head-to tail sequence

H-T

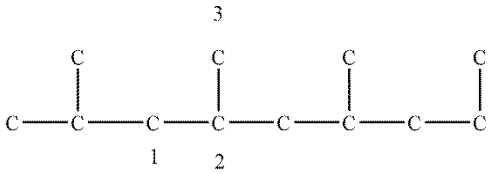

2) Isolated head-to-head regio-error

H-H

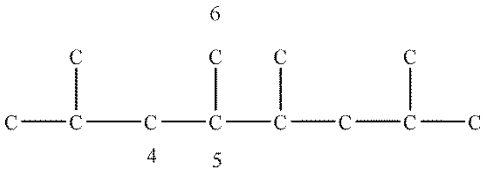

3) Isolated tail-to-tail regio-error

T-T

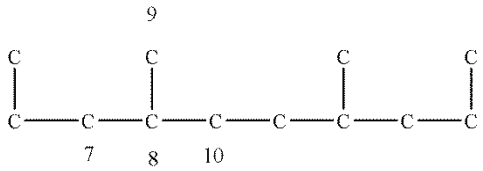

4) Single inverted unit in the head-to tail sequence

1-r

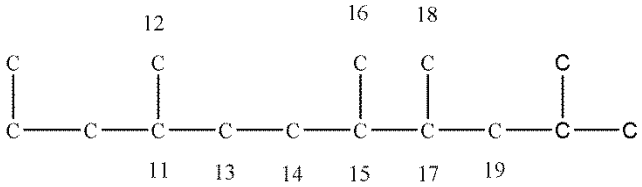

Figure S18. Possible modes of 2,1 insertion during the propylene polymerization**.**

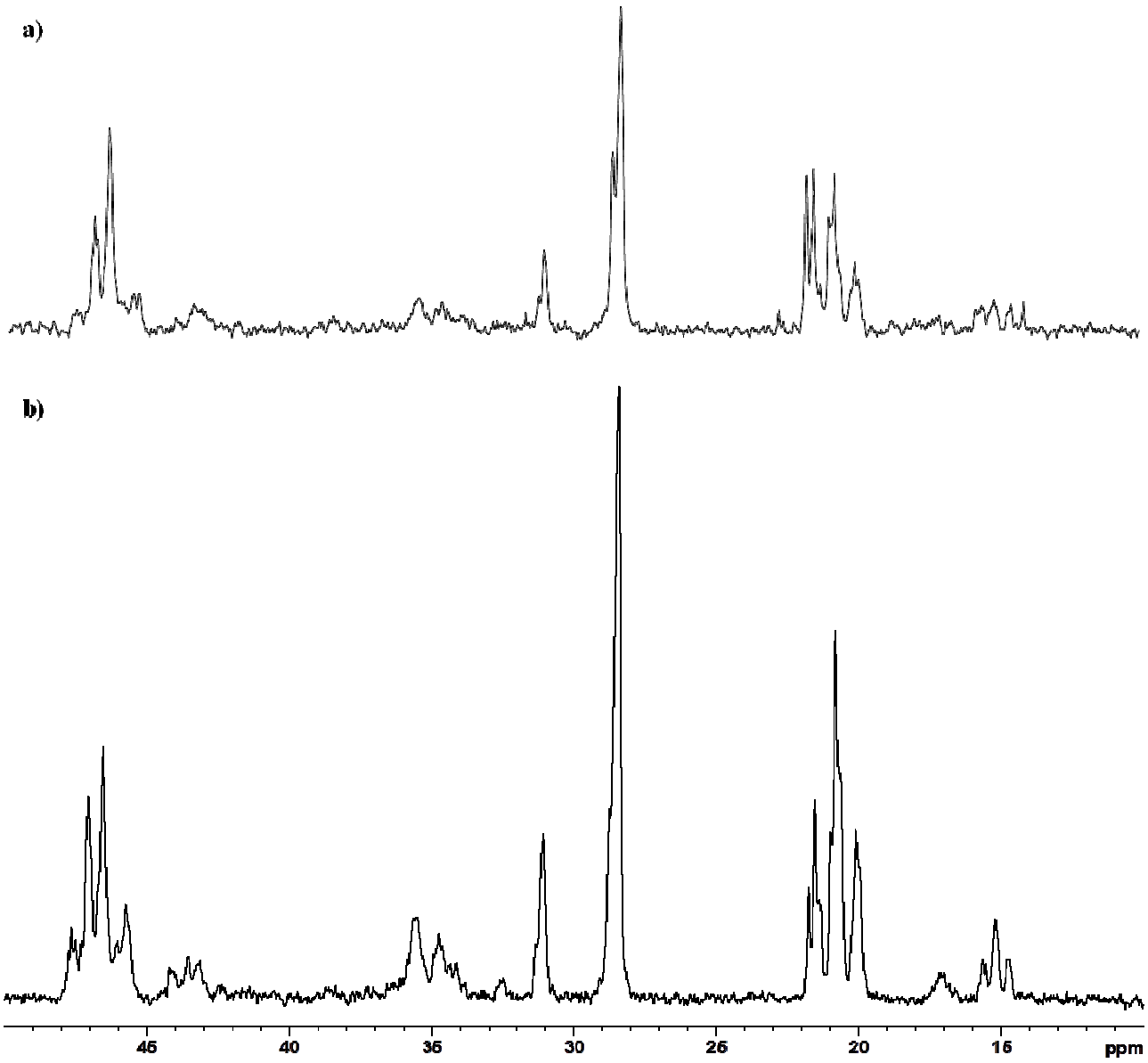

Figure S19 ^{13}C NMR spectra (TCDE, 110 °C, 75 MHz) of polypropylene samples of run 4 (a) and 1 (b) Table 2.

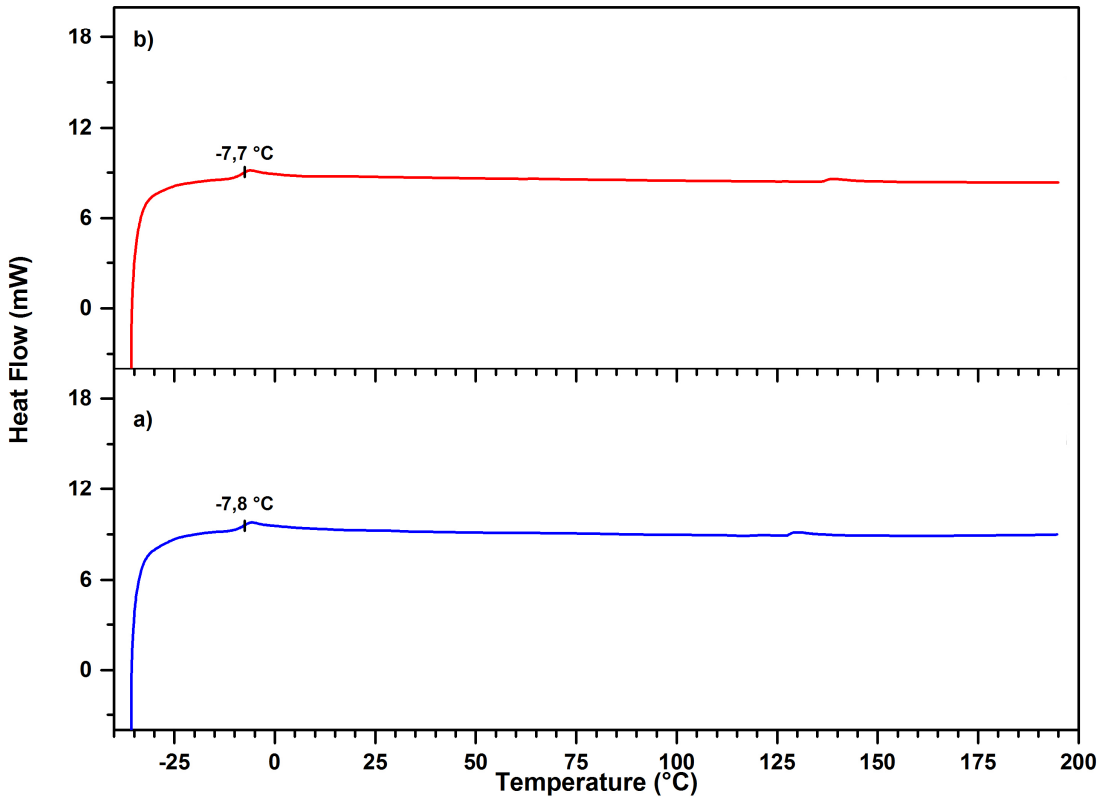

Figure S20. DSC thermograms for polypropylene samples of run 1 (a) and 3 (b) Table 2. Heating rate =10°C min^{-1}

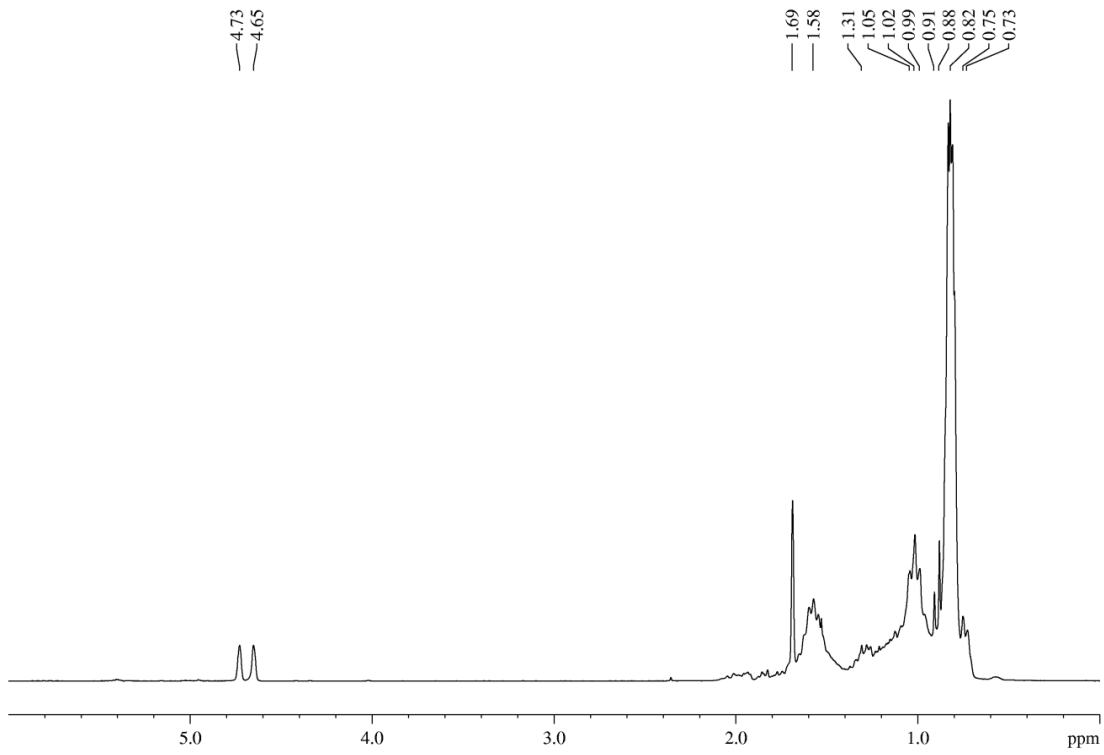

Figure S21. ^{1}H NMR spectrum ($CDCl_3$, 25 °C, 300 MHz) of oligomers obtained from the run 2 Table 2.

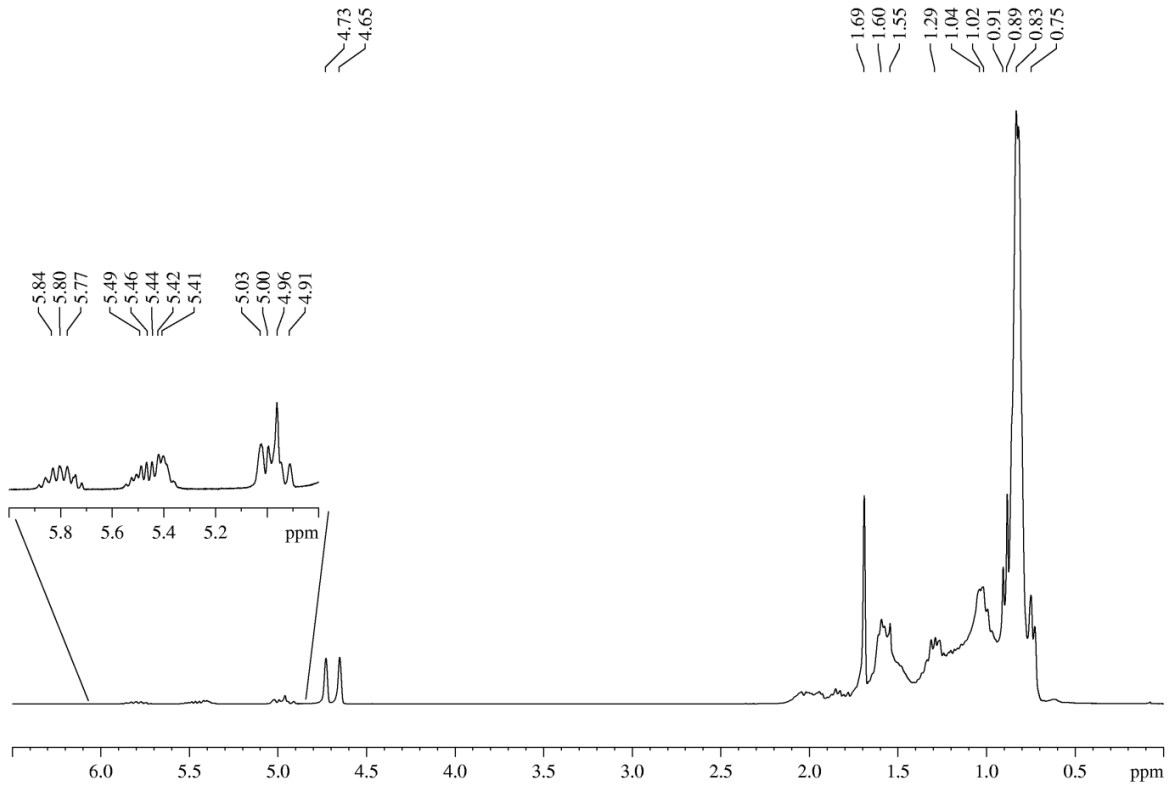

Figure S22. ^{1}H NMR spectrum ($CDCl_3$, 25 °C, 300 MHz) of oligomers obtained from the run 3 Table 2.

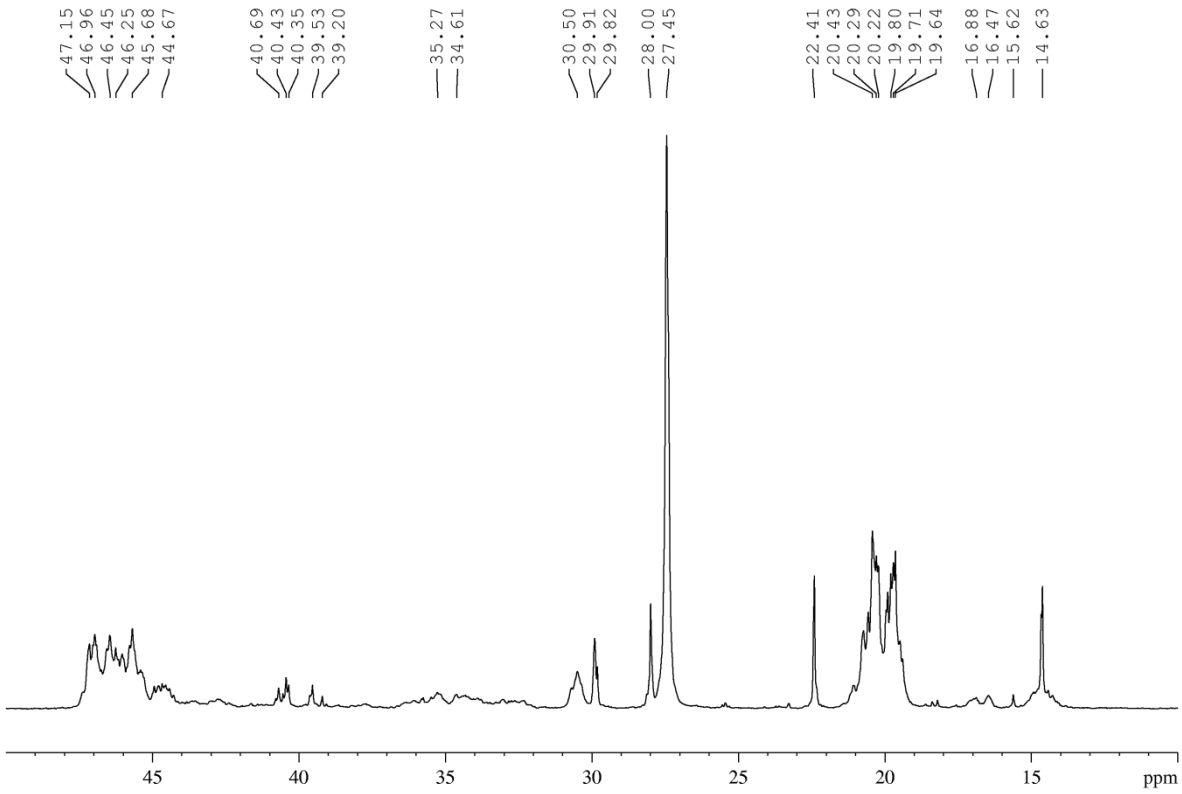

Figure S23. Aliphatic region of ^{13}C NMR spectrum ($CDCl_3$, 25 °C, 75 MHz) of oligomers obtained from the run 2 Table 2.

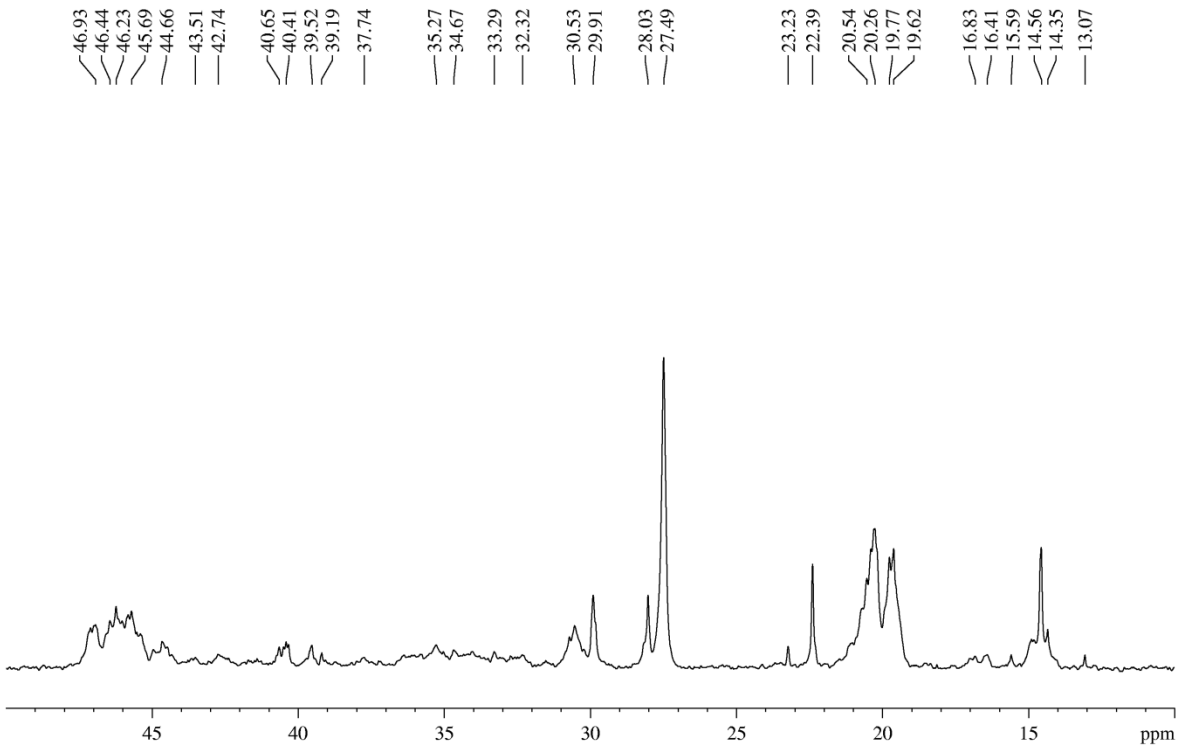

Figure S24. Aliphatic region of ^{13}C NMR spectrum ($CDCl_3$, 25 °C, 75.5 MHz) of oligomers obtained from the run 3 Table 2.

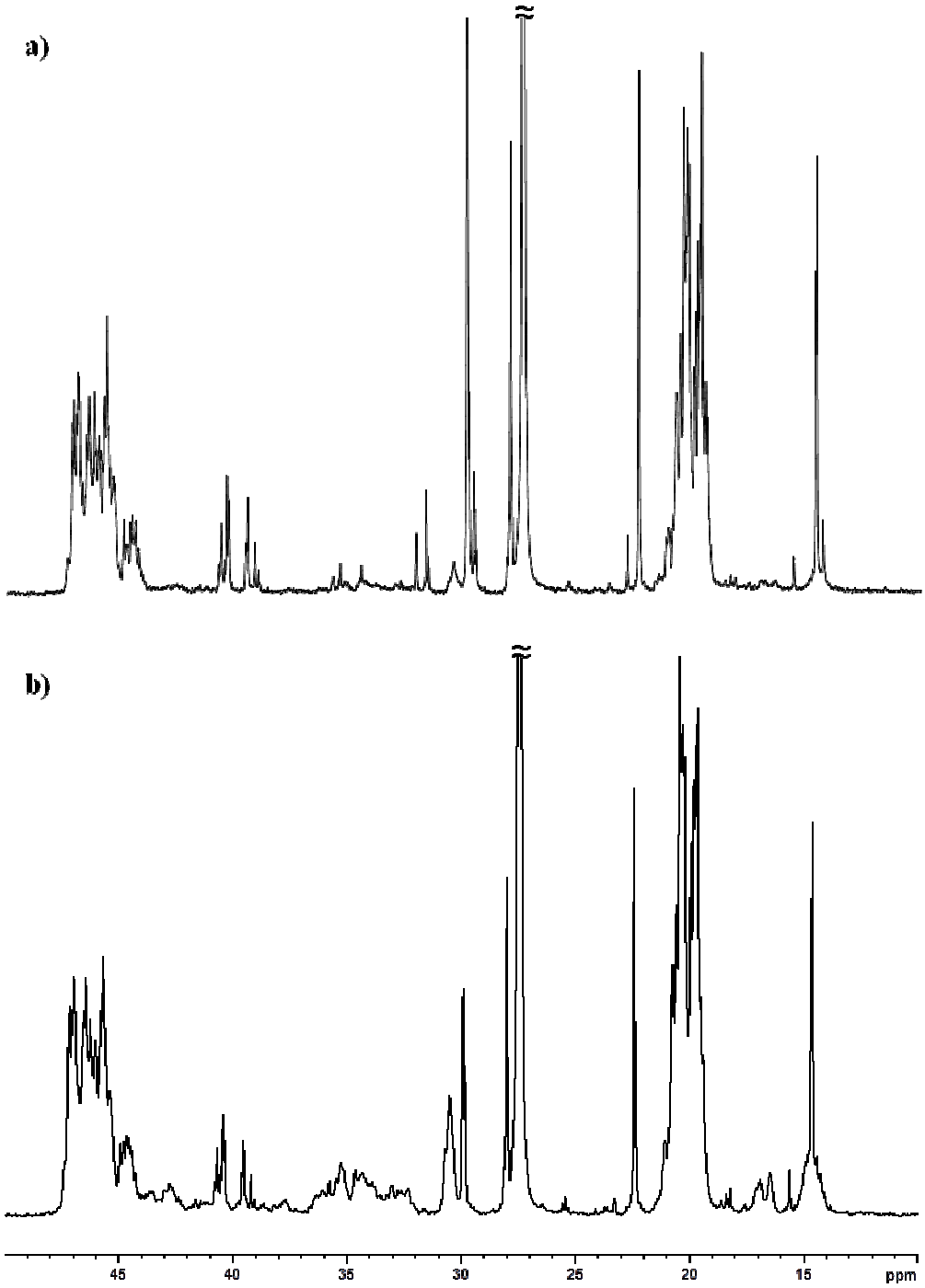

Figure S25. ^{13}C NMR spectra ($CDCl_3$, 25 °C, 75 MHz) of oligomers samples of run 5 (a) and 2 (b) Table 2.

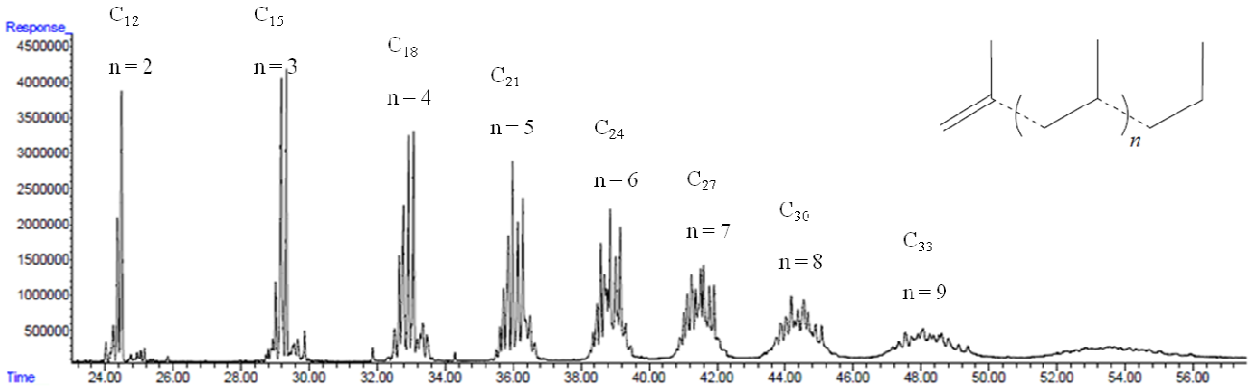

Figure S26. GC trace of the oligomers sample from run 2 Table 2.

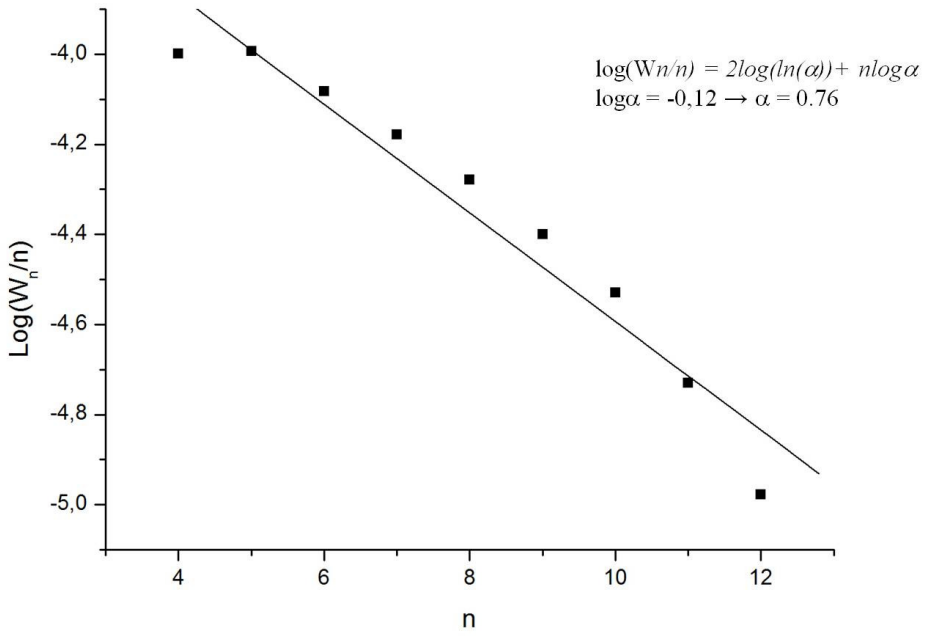

Figure S27. Schulz-Flory distribution of oligomers sample of run 2 Table 2. (R = 0.969).

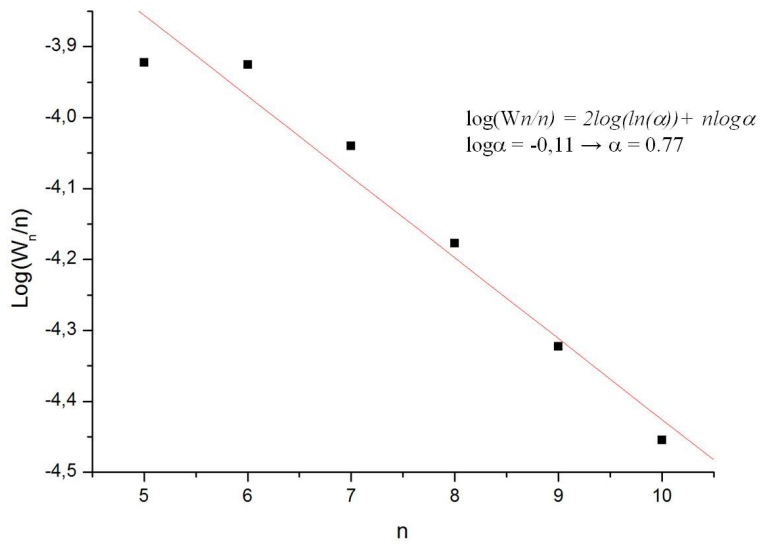

Figure S28. Schulz-Flory distribution of oligomers sample of run 3 Table 2. (R = 0.979).

References

1) T. Asakura, N. Nakayama, M. Demura, A. Asano, *Macromolecules* 1992, **25**, 4876-4881.

2) L. Resconi, L. Cavallo, A. Fait, F. Piemontesi, *Chem. Rev.* 2000, **100**, 1253-1345.